NASA Technical Memorandum 89122

USA AVSCOM Technical Report 87-B-1

The Effects of Crushing Speed on the Energy-Absorption Capability of Composite Material

Gary L. Farley

March 1987

National Aeronautics and Space Administration

Langley Research Center
Hampton, Virginia 23665-5225

THE EFFECTS OF CRUSHING SPEED ON THE ENERGY-ABSORPTION CAPABILITY OF COMPOSITE MATERIAL

by

Gary L. Farley
Aerostructures Directorate
U.S. Army Aviation Research and Technology Activity-AVSCOM
NASA Langley Research Center
Hampton, VA 23665-5225

ABSTRACT

The energy-absorption capability as a function of crushing speed was determined for Thornel 300/Fiberite 934 (Gr/E) and Kevlar-49/Fiberite 934 (K/E) composite material. Circular cross section tube specimens were crushed at speeds ranging from 10^{-2} m/sec to 12 m/sec. Ply orientations of the tube specimens were $[0/\pm\theta]_2$ and $[\pm\theta]_2$ where θ=15, 45, and 75 degrees. Based upon the results of these tests the energy-absorption capability of Gr/E and K/E was determined to be a function of crushing speed. The magnitude of the effects of crushing speed on energy-absorption capability was determined to be a function of the mechanisms that control the crushing process. The crushing modes based upon exterior appearance of the crushed tubes were unchanged for either material. However, the interlaminar crushing behavior of the Gr/E specimens changed with crushing speed.

INTRODUCTION

Composite materials are being proposed for application to aircraft and automotive structures to meet stringent weight and manufacturing cost constraints. Although composite materials can exhibit crushing modes significantly different than the crushing modes of metallic materials recent studies, references 1-11, have shown that composite materials can be efficient energy absorbing materials.

Many studies, references 1, 3, 4, 6, 7, 8, 11-13, have been conducted to investigate how the constitutive material properties of composite materials and specimen architecture effect energy-absorption capability. The majority of these tests have been performed under quasi-static crushing speed conditions to facilitate the understanding of crushing modes and mechanisms while little is understood about the dynamic crushing characteristics.

Limited dynamic crushing tests have been conducted as part of more comprehensive studies reported in references 4, 5, 6, 9, and 11. These dynamic tests were limited in scope and were inconclusive with regards to whether the energy-absorption capability of composite materials is a function of crushing speed. The studies by Hull, references 5 and 9, and Thornton, reference 4, focused primarily on automotive application of composites. The materials evaluated were glass/polyester, glass/epoxy, and graphite/epoxy. A hydraulically actuated test machine was used in the dynamic tests. Crushing speeds

were between quasi-static and 15 m/sec. These studies suggested that glass and graphite reinforced materials were not a function of crushing speed. Farley, reference 8, tested graphite/epoxy, Kevlar/epoxy, and glass/epoxy composite tubular specimens having $[0/\pm\theta]_4$ ply orientation at speeds of quasi-static and 7.6 m/sec. The dynamic tests were conducted in a drop tower. These results suggested that the energy-absorption capability of composite materials was not a function of crushing speed. Bannerman and Kindervater, reference 6, and Kindervater, reference 11, presented test results on Gr/E and K/E tubular and beam specimens. A drop tower was utilized in these studies. The results strongly suggest the energy-absorption capability of composite materials is a function of crushing speed. However, the mechanisms that govern the effects of crushing speed on energy-absorption capability were not identified.

The only study that focused exclusively upon the effects of crushing speed on energy-absorption capability was conducted by Berry and Hull, reference 14. In this study, only [0/90] glass/epoxy fabric tube specimens were evaluated. Crushing speeds were between 10^{-7} and 10 m/sec. Tube specimens had diameter to thickness ratios of 25 and fiber volume fractions of 39 percent. A servo-hydraulic machine was used for the 10 m/sec crushing speed tests while a conventional screw driven test machine was used for all other lower speed tests. The results of this study indicate that energy-absorption capability varies linearly with the log of the crushing speed. A 40 percent increase in energy-absorption capability was obtained between crushing speeds of 10^{-7} m/sec and 10 m/sec. Berry, et. al, reference 14, attributes this phenomena to the effects of strain rate on Mode I crack growth resistance (G_{Ic}). It is reasonable to expect that the energy-absorption trends could be significantly changed with specimens composed of different materials and having different architecture.

The objective of the study reported herein is to determine whether the energy-absorption capability of Thornel 300/Fiberite 934 (Gr/E) and Kevlar 49/Fiberite 934 (K/E) composite material is a function of crushing speed and to develop an understanding of the crushing mechanisms. Circular cross section tubular specimens were crushed between speeds of 10^{-2} m/sec and 12 m/sec. Crushing speed was maintained constant, within the capability of the test machine, as the specimens were crushed. Ply orientations investigated were $[0/\pm\theta]_2$ and $[\pm\theta]_3$. The crushing force and speed as a function of time were recorded for each specimen. An investigation of the crushing mechanisms of the Gr/E and K/E was performed. A closed loop hydraulic actuated test system was used to test specimens.

TEST SPECIMEN

Circular cross section tubes were used as test specimens because of their inherent stability, ease of fabrication, and for comparison with previous data. Tubes nominally 20.3 cm in length by 3.81 cm inside diameter were used, figure 1. One end of each tube was chamfered so crushing could be initiated without causing catastrophic failure of the specimen.

Tube specimens were fabricated using unidirectional prepreg of Thornel 300/Fiberite 934 (Gr/E) and Kevlar-49/Fiberite 934 (K/E). Nominal cured ply

thickness of the tape prepreg is 0.013 cm (0.005 in). Prepreg material was wrapped around a metal mandrel using a table wrapper. Tubes were overwrapped with a peel ply, shrink tubing was slipped over the peel ply, and the assembly was placed in an oven to cure at 176°C.

Tube ply orientations of $[0/\pm\theta]_2$ and $[\pm\theta]_3$ where θ=15, 45, and 75 degrees were evaluated. Tables 1 and 2 present detail information on each tube tested along with the test conditions.

TEST EQUIPMENT, PROCEDURES AND DATA ANALYSIS

Tube specimens were crushed at speeds in excess of 0.01 m/sec using a closed loop hydraulically operated impact system (CLHOIS). A conventional static hydraulically operated test machine was used for tests where crushing speeds were less than 0.01 m/sec. The CLHOIS, figures 2 and 3, provided constant crushing speeds from 0.01 m/sec to 12 m/sec. Maximum crushing force in the CLHOIS was 22 kN. Crushing force and ram speed as a function of time were recorded on a high speed storage tube oscilloscope. All force and speed data were subsequently stored on a removable mass storage device (floppy diskette) for later analysis.

A 21 MPa hydraulic power supply provided the means to propel the ram and crushing apparatus at the required speed. The desired crushing speed was set prior to each test. A ram fire order was initiated and hydraulic pressure accelerates the ram to the specified speed. The hydraulic feed back loop was closed by a speed transducer feeding back ram speed to a signal conditioner. Actual ram speed was compared with specified values to produce any necessary changes in ram speed. The acceleration of the ram to the specified speed was performed within 10.2 cm of ram travel. Figure 4 depicts a representative ram speed profile.

After the ram traversed the 10.2 cm acceleration phase and the set speed was reached, the sliding load platen contacts the impact plate. The stationary platen is mounted to the ram. Tube specimens are positioned between the stationary and sliding platens, figure 3. The load cell is mounted in line with the hydraulic ram. When the sliding platen impacts the impact plate, the tube specimen is crushed between the sliding and stationary platens. The tubes were crushed at a constant crushing speed for approximately 10.2 cm. Entrapped air escape holes were incorporated into the design of the sliding platen to minimize any air spring effects that could occur during the dynamic crushing of a tube specimen.

The procedure for testing a tube consisted of first mounting the tube in the crushing apparatus. The chamfered end was always positioned adjacent to the sliding platen. The required impact speed was set and the storage oscilloscope was readied. An electronic trigger on the oscilloscope was set to trigger prior to the inital impact of the sliding platen and the impact plate. The CLHOIS and oscilloscope are readied and the system was fired.

The test data stored in the oscilloscope were transferred to a floppy diskette for subsequent analysis. From each test ram speed and crushing force profiles as a function of time were developed similar to those depicted in figure 5.

Approximately 2000 data points, evenly spaced in time, were recorded per ram speed and crushing force data channel. Within the time interval corresponding to a relatively constant velocity and uniform crushing response, the maximum, minimum, and average crushing force and ram speed were determined.

All test data were reduced to a specific sustained crushing stresses for comparative purposes. The specific sustained crushing stress is the average crushing force, as depicted in figure 5, divided by the product of the cross-sectional area and density of the tube. Cross-sectional area and density of the tube are used to account for differences in tube architecture. Test data are presented as the specific sustained crushing stress plotted on the ordinate axis as a function of crushing speed.

RESULTS AND DISCUSSION

Crushing Process

The effects of crushing speed on the energy-absorption capability of a specimen are related to whether the matrix and/or fiber mechanical properties are a function of strain rate. Inertial effects have been attributed to differences in static and dynamic response of metallic floor structures, reference 15. However, the inertial effects produced significantly different crushing modes of the structure than were obtained in the static tests. To better understand how crushing speed effects energy-absorption capability it is necessary to examine the mechanisms that control the crushing process and determine how crushing speed effects these mechanisms.

The controlling mechanisms exhibited by the four crushing modes are: transverse laminate strength (transverse shearing crushing mode), matrix strength (brittle fracturing crushing mode and lamina bending crushing modes), lamina bundle bending strength (brittle fracturing crushing mode), and fiber/matrix yield strength (local buckling crushing mode). The transverse strength of a laminate is primarily a function of fiber strength. Therefore, if the fibers mechanical response is a function of strain rate then the energy-absorption capability of specimens that crush in a transverse shearing mode can be a function of crushing speed.

The matrix strength controls the interlaminar crack growth in both the brittle fracturing and lamina bending crushing modes. Many polymeric-matrix materials exhibit mechanical responses that are a function of strain rate. Therefore, a specimen that exhibits either the brittle fracturing mode or lamina bending mode can exhibit energy-absorption capability that is a function of crushing speed. The effects of crushing speed on energy-absorption capability occur when the percentage of energy absorbed by the interlaminar crack growth is a significant part of the total energy absorbed. Specimens that crush in the lamina bending mode will more readily exhibit energy-absorption capability that is a function of crushing speed than specimens that crush in the brittle fracturing mode. In the lamina bending crushing mode, a significant portion of the total energy absorbed is by interlaminar crack growth, whereas a much smaller portion of the energy is absorbed by interlaminar crack growth in the brittle fracturing crushing mode.

The bending strength of the lamina bundle controls the fracturing of the lamina bundle in the brittle fracturing crushing mode. The mechanical response of the lamina bundle is primarily a function of either fiber (e.g., 0 degree lamina bundle) or matrix (e.g., 90 degree lamina bundle or low fiber volume fraction material). Therefore, if the mechanical response of the dominant property (fiber or matrix) is a function of strain rate then the fracturing of the lamina bundle and hence the energy-absorption capability can be a function of crushing speed.

The mechanism that controls the local buckling crushing mode is the yield strength of the fiber and/or matrix. Brittle fiber reinforced composites can produce the local buckling crushing mode only if the matrix has a low stiffness and high failure strain. Therefore, if the matrix mechanical response is a function of strain rate then the energy-absorption capability can be a function of crushing speed. Ductile fiber reinforced composites crush in the local buckling mode because of either the fiber or matrix properties. Therefore, if either the fibers or matrices mechanical response is a function of strain rate then the energy-absorption capability can be a function of crushing speed.

Graphite/Epoxy Tube Specimens

The energy-absorption capability of $[0/\pm\theta]_2$ Gr/E specimens was not a function of crushing speed as shown in figure 6. All specimens crushed in a brittle fracturing mode. The energy associated with the fracturing of the lamina bundles is considerably more than the energy associated with interlaminar crack growth in the brittle fracturing mode. All $[0/\pm\theta]_2$ specimens have 0 degree plies in the layup. The 0 degree plies in the lamina bundle reduce strain rate effects of the mechanical response. Therefore, the energy-absorption capability of $[0/\pm\theta]_2$ specimens should not be a function of the crushing speed which is consistent with the results depicted in figure 6.

The energy-absorption capability of $[\pm\theta]_3$ Gr/E specimens was a function of crushing speed as shown in figure 6. As ply orientation angle, θ, increased from 15 to 75 degrees the magnitude of the effects of crushing speed on energy-absorption capability increased. Energy-absorption capability increased as much as 35 percent over the speed ranged tested. All $[\pm\theta]_3$ specimens crushed in predominantly a brittle fracturing mode. As the ply orientation angle increased from 45 to 75 degrees the mechanical response of the lamina bundles became more strongly influenced by the matrix properties than the fiber properties. The percent of the total energy absorbed by the fracturing of the lamina bundles decreased, therefore, the energy absorbed by the interlaminar crack growth relative to the total energy absorbed increased. If the matrix mechanical response is a function of strain rate, then the energy-absorption capability of the specimen is a function of crushing speed. The magnitude of the change in energy-absorption capability is a function of ply orientation angle.

Figure 7 depicts typical Gr/E crushed tubes having ply orientations of $[0/\pm45]_2$ and $[\pm45]_3$ crushed at speeds of 0.01 m/sec, 6 m/sec and 12 m/sec. Based upon the exterior appearance of the tube the crushing response was not a function of crushing speed. After sectioning the tube specimens and examining the crushing mode more closely, differences in crushing behavior

were distinguishable. Figure 8 shows photomicrographs depicting the crushing behavior of $[0/\pm45]_2$, $[0/\pm75]_2$, $[\pm45]_3$, and $[\pm75]_3$ specimens. The characteristic cracking pattern of the $[0/\pm\theta]_2$ specimens, "as seen" in figure 8, is the formation of interlaminar cracks adjacent to the 0 degree plies. These interlaminar cracks form lamina bundles which fail in a brittle fracturing mode. The length of the interlaminar cracks of the $[0/\pm45]_2$ specimens were similar for the 0.01 m/sec and the 12 m/sec cases, and the energy-absorption capabilities were comparable. However, the interlaminar cracks of the 6 m/sec cases for the $[0/\pm45]_2$ specimen was shorter than those for the other crushing speed. The $[0/\pm75]_2$ specimen exhibited less interlaminar cracks at 0.01 m/sec than the 6 m/sec and 12 m/sec cases. The growth in interlaminar cracks with crushing speed is a function of the matrix mechanical response being a function of strain rate similar to that reported in reference 14.

Kevlar/Epoxy Tube Specimens

Figure 9 shows the effect of crushing speed on the energy-absorption capability of $[0/\pm\theta]_2$ and $[\pm\theta]_2$ K/E tube specimens. All K/E tube specimens crushed in the local buckling mode. The energy-absorption capability of all K/E specimens was determined to be a function of crushing speed particularly between crushing speeds of 6 m/sec and 12 m/sec. Energy-absorption capability increased between 20 and 45 percent for both $[0/\pm\theta]_2$ and $[\pm\theta]_3$ specimens between crushing speeds of 10^{-2} m/sec and 12 m/sec. Specimens with fibers predominantly oriented in the direction of the applied load (e.g., $[0/\pm15]_2$ and $[\pm15]_3$) exhibited the most significant increase in energy-absorption capability as crushing speed increased from 6 m/sec to 12 m/sec. The mechanical response of Kevlar fibers is a function of strain rate as a result of the polymer origin of the fiber. Therefore, the observed change in energy-absorption capability with changes in crushing speed and ply orientation are reasonable.

Figure 10 depicts typical crushing behavior of the K/E tubes. All K/E specimens exhibited the characteristic local buckling mode. No noticable change in crushing modes were evident between different crushing speeds.

General

The results describing the effect of crushing speed on $[0/\pm\theta]_2$ and $[\pm\theta]_3$ Gr/E and K/E is consistent with the crushing process described in a previous section. Specimens whose crushing mechanisms' mechanical response is a function of strain rate exhibited an energy-absorption capability that was a function of crushing speed.

CONCLUDING REMARKS

Graphite/epoxy (Gr/E) and Kevlar/epoxy (K/E) tube specimens with ply orientations of $[0/\pm\theta]_2$ and $[\pm\theta]_3$ were crushed at crushing ram speeds between 10^{-2} m/sec and 12 m/sec. The energy-absorption capabilities and crushing modes were determined as a function of crushing speed. The effects of crushing speed on the energy-absorption capability of specimens fabricated from composite material was determined to be related to whether the mechanical response of the crushing mechanism that controls the crushing process is a

function of strain rate. The energy-absorption capability of the $[0/\pm\theta]_2$ Gr/E specimens were not a function of crushing speed while the $[\pm\theta]_3$ Gr/E specimens exhibited up to a 35 percent change in energy-absorption capability. The magnitude of the change in energy-absorption capability with respect to change in crushing speed of the $[\pm\theta]_3$ Gr/E specimens was a function of ply orientation. Both $[0/\pm\theta]_2$ and $[\pm\theta]_3$ K/E specimens exhibited between 20 and 45 percent increase in energy-absorption capability. Furthermore, the percent change in energy-absorption capability with respect to crushing speed was directly related to the amount of Kevlar fiber oriented in the direction of the applied load.

REFERENCES

1. Thornton, P. H.: Energy Absorption in Composite Structures. Journal of Composite Materials, vol. 13, July 1979.

2. Cronkhite, J. D., Hass, T. J., Berry, V. L., and Winter, R.: Investigation of the Crash Impact Characteristics of Advanced Airframe Structure. USARTL-TR-79-11, Sept. 1979.

3. Kindervater, C. M.: Quasi-Static and Dynamic Crushing of Energy-Absorbing Materials and Structural Components With the Aim of Improving Helicopter Crashworthiness. Seventh European Rotorcraft and Powered Lift Aircraft Forum, Sept. 1981.

4. Thornton, P. H., and Edwards, P. J.: Energy Absorption in Composite Tubes. Journal of Composite Materials, vol. 16, Nov. 1982.

5. Hull, D.: Energy Absorption of Composite Materials Under Crash Conditions. Proceedings of ICCM-IV, 1982.

6. Bannerman, D. C. and Kindervater, C. M.: Crash Energy Absorption Properties of Composite Structural Elements. Proceedings of Fourth International Conference and Exhibition, Oct. 1983.

7. Kindervater, C. M.: Energy Absorbing Qualities of Fiber Reinforced Plastic Tubes. National Specialists Meeting Composite Structures of the American Helicopter Society, March 1983.

8. Farley, G. L.: Energy Absorption of Composite Materials. Journal of Composite Materials, vol. 17, May 1983.

9. Hull, D.: Research on Composite Materials at Liverpool University, Part 2: Energy Absorbing Composite Materials. Physics Technology, vol. 14, 1983.

10. Sen, J. K.: Designing for a Crashworthy All-Composite Helicopter Fuselage. Presented at 40th Annual Forum of the American Helicopter Society, May 1984.

11. Kindervater, C. M.: Compression and Crush Energy Absorption Behavior of Composite Laminates. Proceedings of E/MRS Conference on Advanced Materials Research and Development for Transport, Nov. 1985.

12. Farley, G. L.: Effect of Fiber and Matrix Strain on the Energy Absorption of Composite Materials. Journal of Composite Materials, vol. 20, no. 4, July 1986.

13. Farley, G. L.: Effect of Specimen Geometry on the Energy Absorption Capability of Composite Materials. Journal of Composite Materials, volume 20, no. 4, July 1986.

14. Berry, J. and Hull, D.: Effect of Speed on Progressive Crushing of Epoxy-Glass Cloth Tubes. Institute Physics Conference on the Mecanical Properties at High Rates of Strain, 1984.

15. Carden, H. D. and Hayduk, R. J.: Aircraft Subfloor Response to Crash Loadings. SAE Paper No. 810614, Apr. 1981.

Table 1. Graphite/Epoxy Composite Tube Specimens.

Specimen Description		Weight, Grams	Wall Thickness CM	Crushing Speed M/Sec	Specimen Description		Weight, Grams	Wall Thickness CM	Crushing Speed M/Sec
$[\pm 45]_3$	1	32.5	0.081	0.021	$[0/\pm 45]_2$	1	32.5	0.078	0.012
	2	33.0	0.081	0.021		2	32.3	0.081	0.012
	3	32.8	0.084	0.021		3	32.6	0.081	0.012
	4	32.1	0.084	5.91		4	32.5	0.081	TMM*
	5	32.8	0.084	5.91		5	32.4	0.078	5.72
	6	32.7	0.084	5.91		6	31.8	0.076	5.72
	7	33.1	0.084	12.36		7	32.7	0.076	11.95
	8	33.1	0.084	12.36		8	32.3	0.076	11.95
	9	32.6	0.084	12.36		9	32.1	0.078	11.95
$[\pm 75]_3$	1	32.6	0.086	0.02	$[0/\pm 75]_2$	1	32.3	0.081	0.012
	2	33.0	0.086	0.02		2	32.6	0.078	0.012
	3	33.0	0.086	0.02		3	32.2	0.083	0.012
	4	33.2	0.086	5.80		4	32.7	0.083	5.92
	5	33.5	0.086	5.80		5	32.5	0.078	5.92
	6	32.9	0.086	5.80		6	33.1	0.078	5.92
	7	33.6	0.089	12.19		7	33.0	0.081	12.36
	8	32.7	0.086	12.19		8	32.6	0.078	12.36
	9	33.0	0.086	12.19		9	32.2	0.078	12.36

TMM* - Test Machine Malfunction

Table 2. Kevlar/Epoxy Composite Tube Specimens.

Specimen Description		Weight, Grams	Wall Thickness CM	Crushing Speed M/Sec	Specimen Description		Weight, Grams	Wall Thickness CM	Crushing Speed M/Sec
$[\pm 15]_3$	1	28.0	0.078	0.018	$[0/\pm 15]_2$	1	28.3	0.076	0.012
	2	27.9	0.076	0.018*		2	27.6	0.076	0.012
	3	27.7	0.074	DAE*		3	28.6	0.081	0.012
	4	28.0	0.081	4.88		4	27.1	0.073	6.31
	5	27.7	0.076	4.88		5	28.6	0.076	6.31
	6	28.1	0.076	4.88		6	28.0	0.083	6.31
	7	27.9	0.074	13.28		7	27.9	0.083	13.35
	8	27.4	0.076	13.28		8	28.0	0.086	13.35
	9	27.8	0.074	13.28		9	27.5	0.078	13.35
$[\pm 45]_3$	1	27.3	0.081	0.018	$[0/\pm 45]_2$	1	28.0	0.086	0.012
	2	27.2	0.086	0.018		2	27.9	0.086	0.012
	3	27.1	0.081	0.018		3	27.2	0.081	0.012
	4	26.9	0.081	6.13		4	27.9	0.084	6.31
	5	27.8	0.086	6.13		5	28.0	0.089	6.31
	6	27.4	0.084	6.13		6	28.0	0.081	6.31
	7	27.5	0.089	13.15		7	28.2	0.094	13.09
	8	27.5	0.081	13.15		8	28.5	0.084	13.09
	9	27.1	0.089	13.15		9	27.8	0.084	13.09
$[\pm 75]_3$	1	26.6	0.096	0.018	$[0/\pm 75]_2$	1	27.8	0.081	0.012
	2	28.0	0.091	DAE		2	28.3	0.081	0.012
	3	27.8	0.089	DAE		3	27.7	0.084	0.012
	4	27.8	0.107	6.12		4	28.0	0.089	5.97
	5	27.0	0.089	6.12		5	27.7	0.089	5.97
	6	27.6	0.089	6.12		6	27.4	0.084	5.97
	7	27.9	0.089	13.05		7	27.4	0.089	12.85
	8	27.9	0.089	13.05		8	27.3	0.089	12.85
	9	27.3	0.086	13.05		9	27.3	0.091	12.85

DAE* - Data Acquisition System Error

SKETCH OF TYPICAL COMPOSITE TUBE SPECIMEN

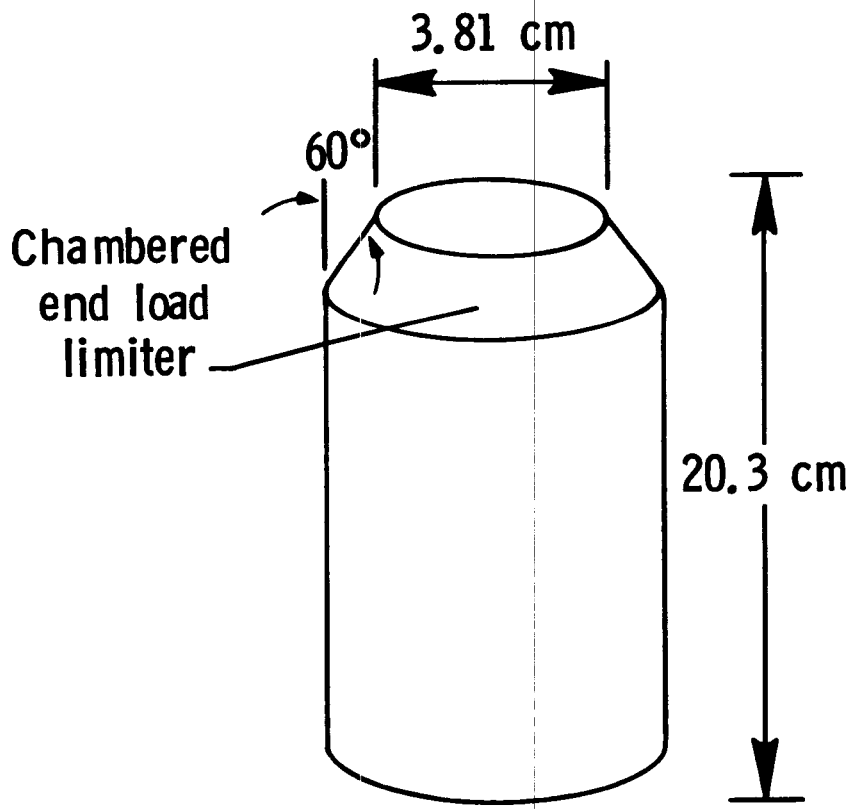

Figure 1. Sketch of typical composite tube specimen.

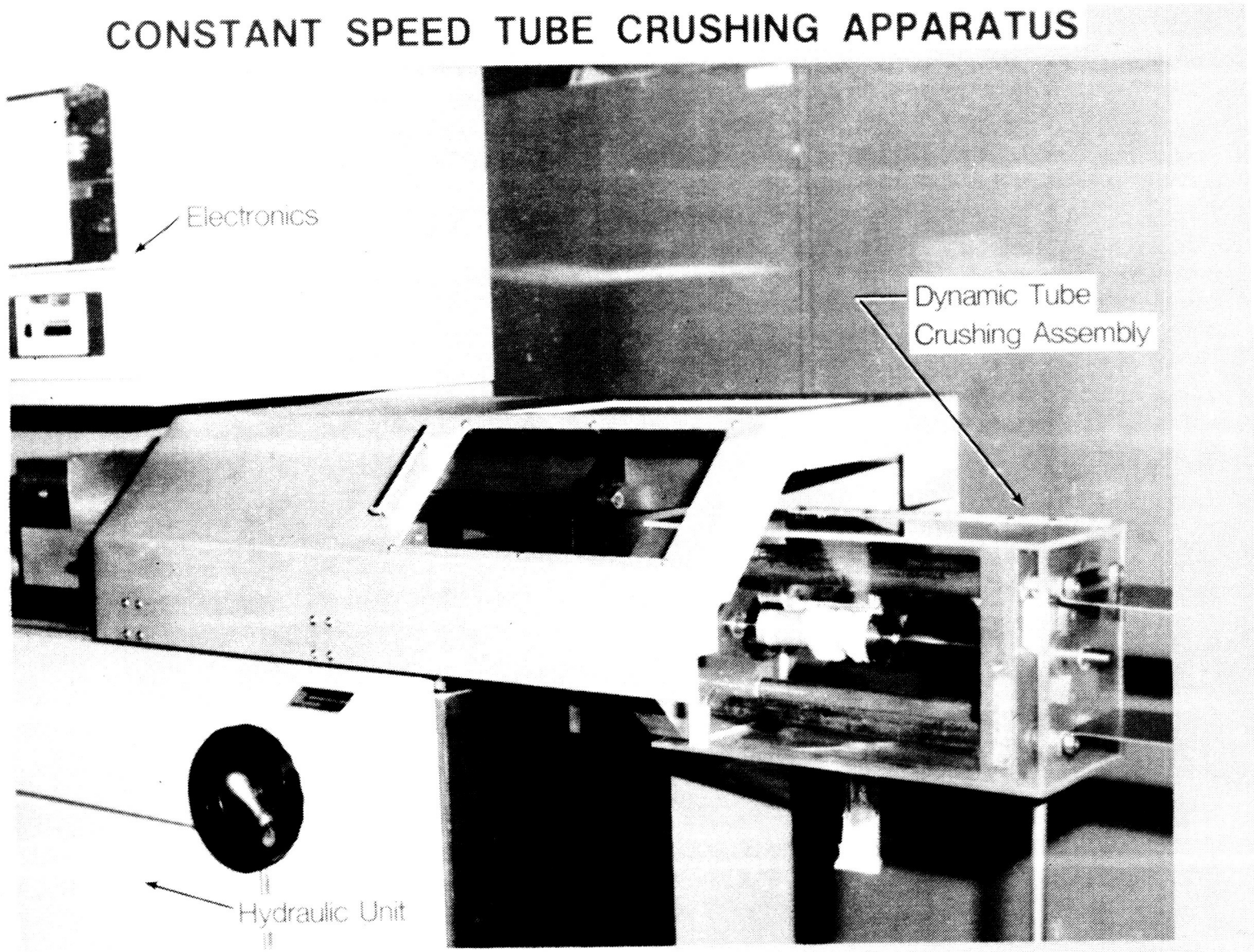

Figure 2. Constant speed tube crushing apparatus.

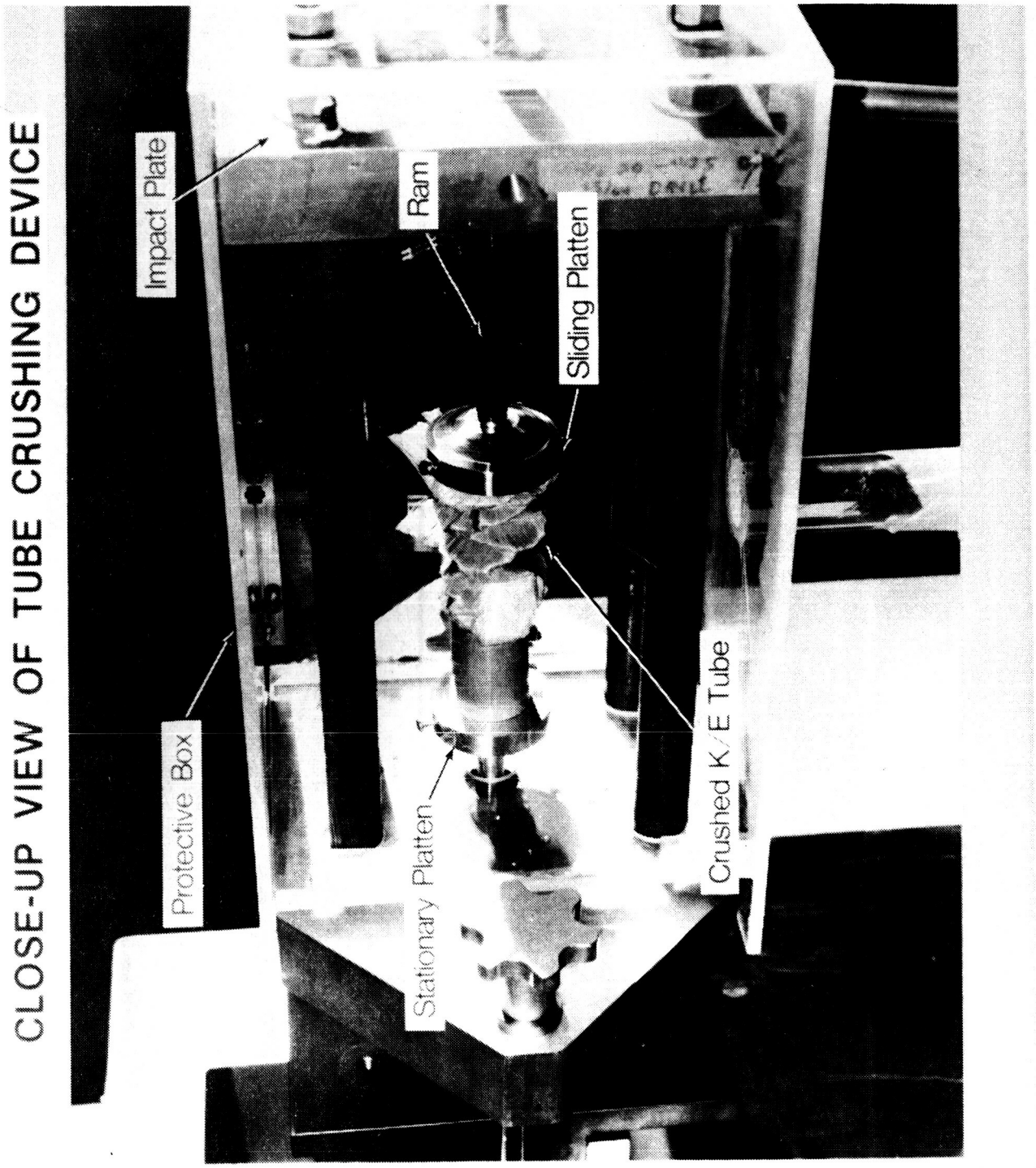

Figure 3. Close-up view of tube crushing device.

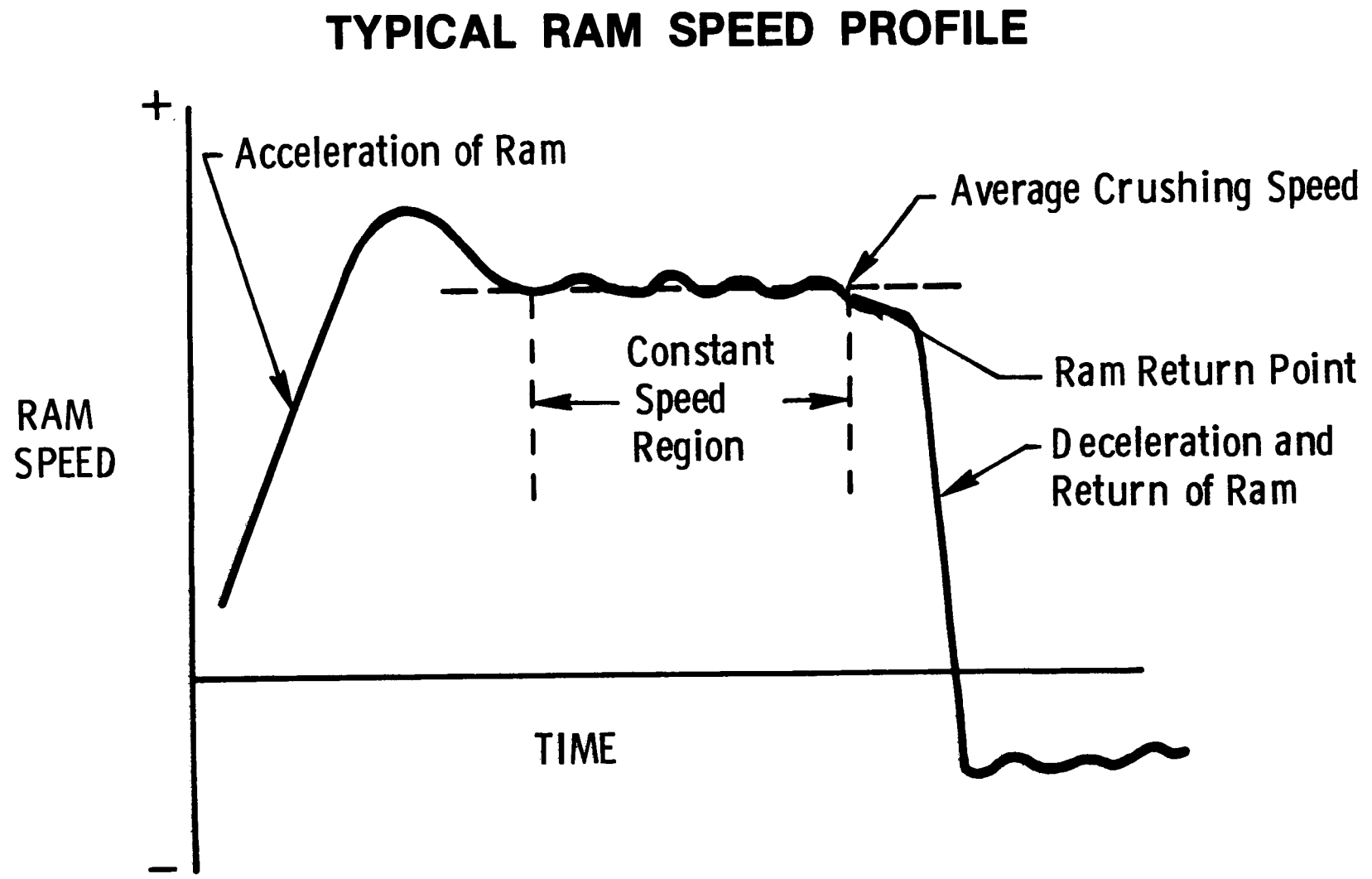

Figure 4. Typical ram speed profile.

TYPICAL RAM SPEED AND CRUSHING FORCE PROFILES

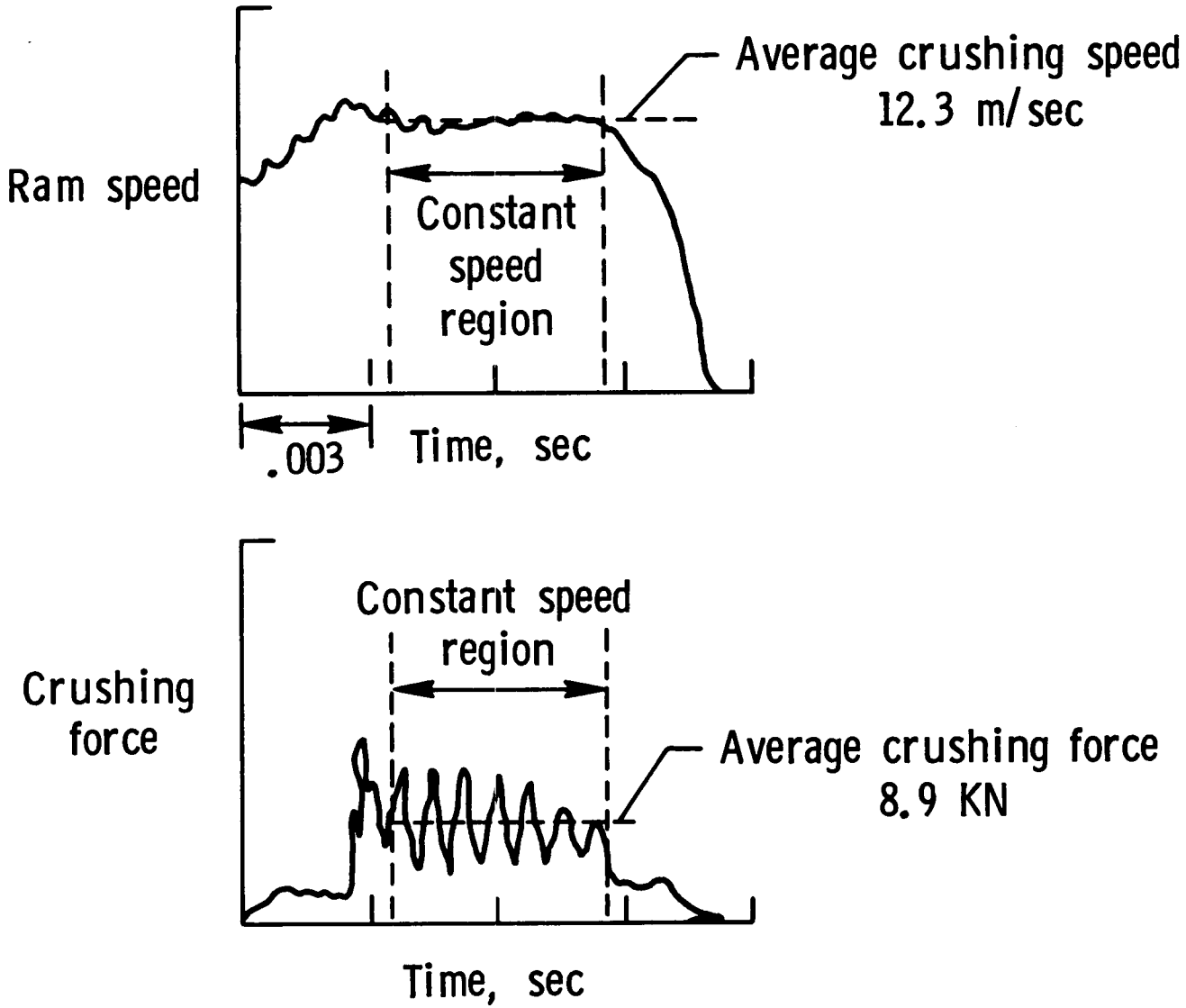

Figure 5. Typical ram speed and crushing force profiles of $[\pm 45]_3$ graphite/epoxy specimen.

EFFECTS OF CRUSHING SPEED ON Gr/E TUBES

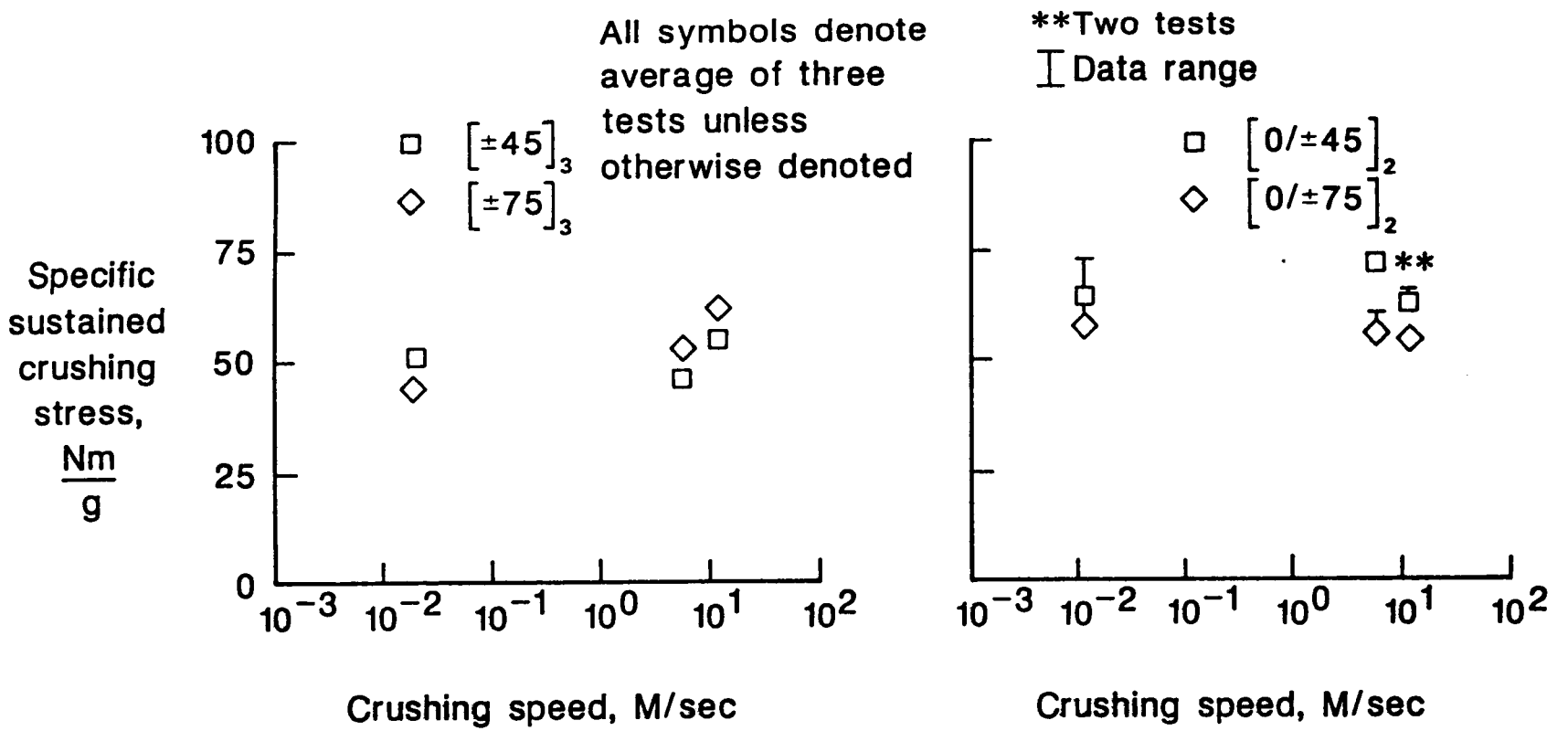

Figure 6. Effects of crushing speed on energy absorption capability of $[0/\pm\theta]_2$ and $[\pm\theta]_3$ graphite/epoxy tubes.

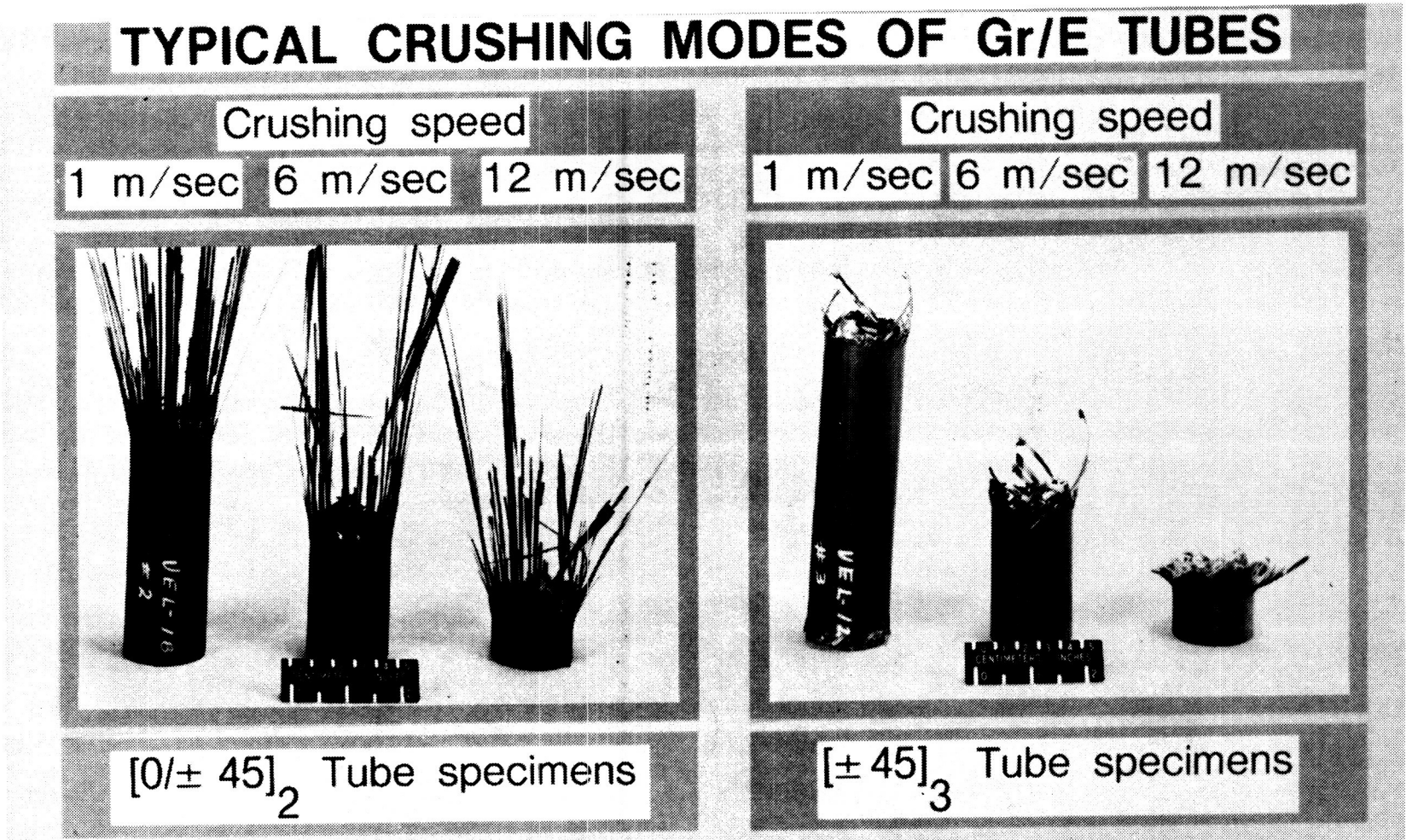

Figure 7. Typical crushed graphite/epoxy tubes at crushing speeds of quasi-static, 6 m/sec, and 12 m/sec.

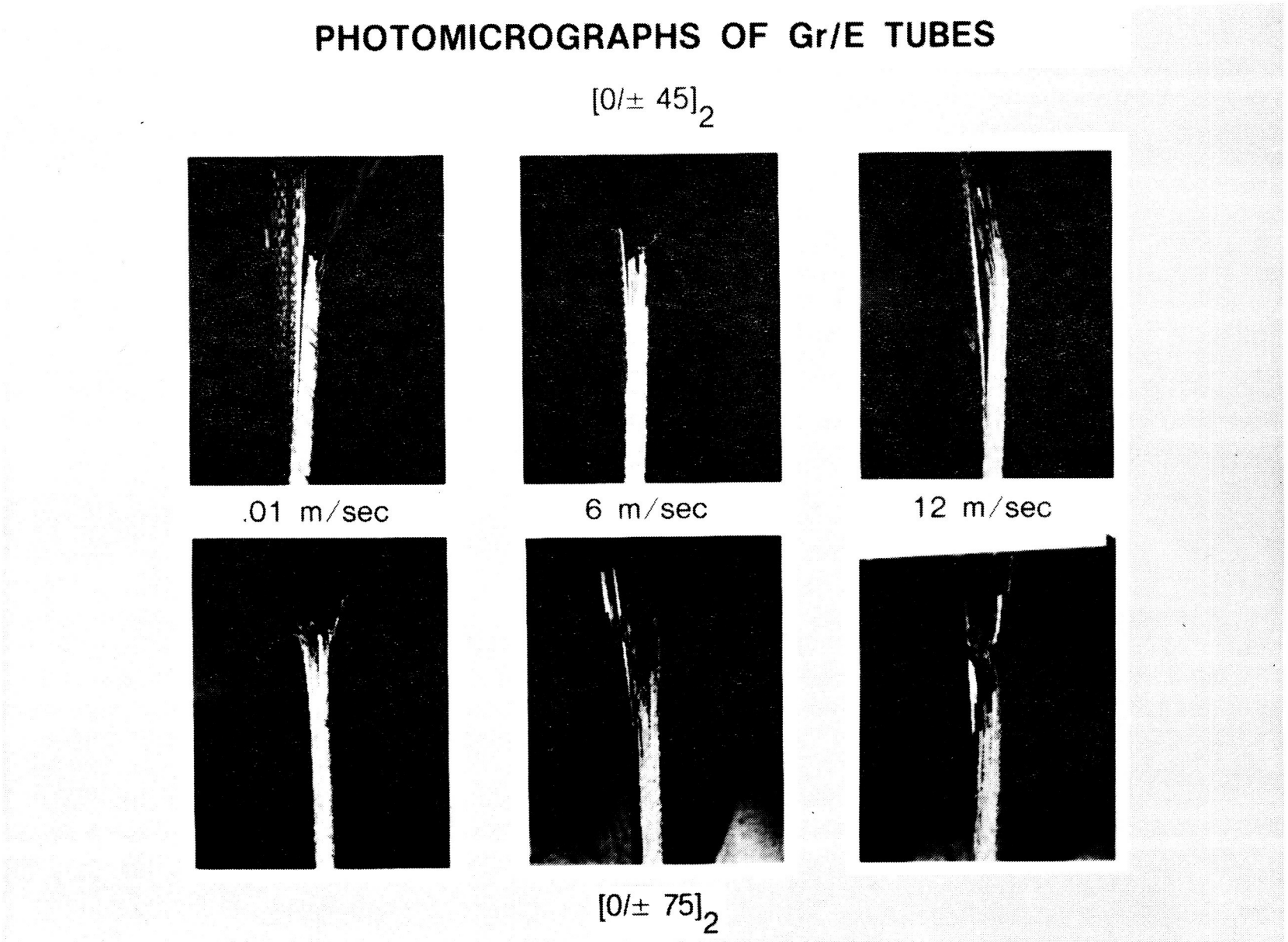

Figure 8. Photomicrographs of crushed $[0/\pm45]_2$, $[0/\pm75]_2$, $[\pm45]_3$, and $[\pm75]_3$ graphite/epoxy specimens(Continued).

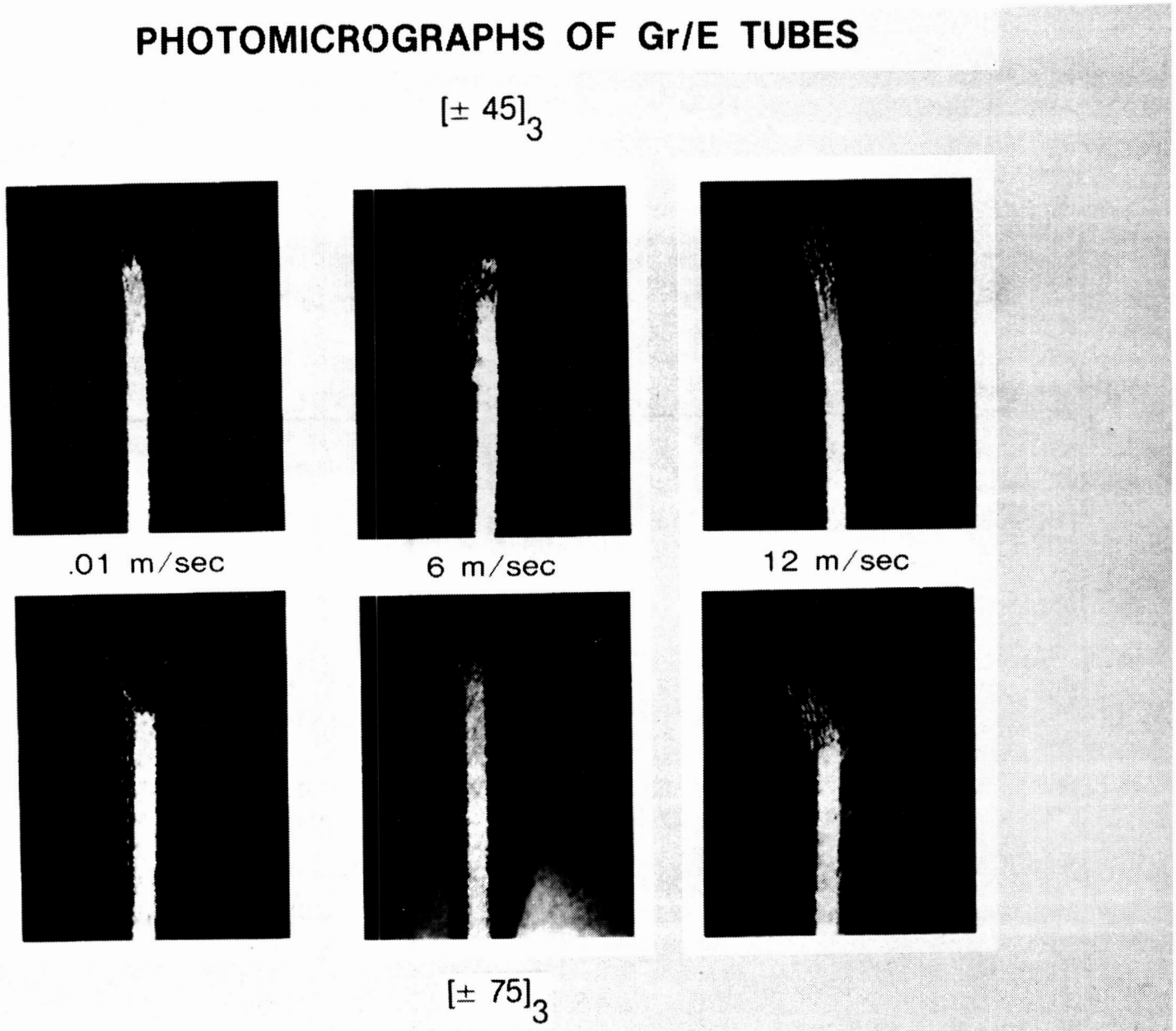

Figure 8. Photomicrographs of crushed $[0/\pm45]_2$, $[0/\pm75]_2$, $[\pm45]_3$, and $[\pm75]_3$ graphite/epoxy specimens (Concluded).

EFFECTS OF CRUSHING SPEED ON K/E TUBES

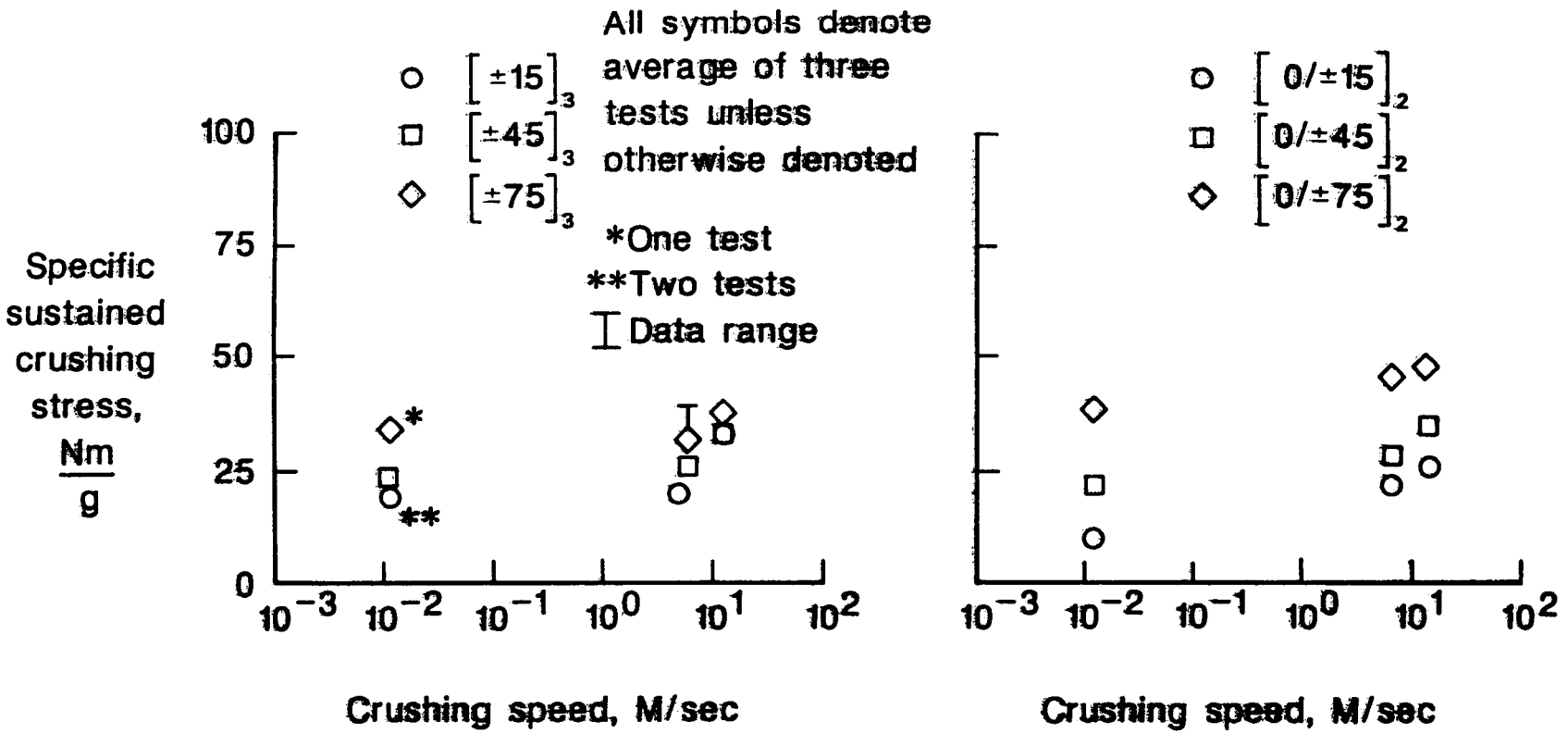

Figure 9. Effects of crushing speed on energy absorption capability of $[0/\pm\theta]_2$ and $[\pm\theta]_3$ Kevlar/epoxy tubes.

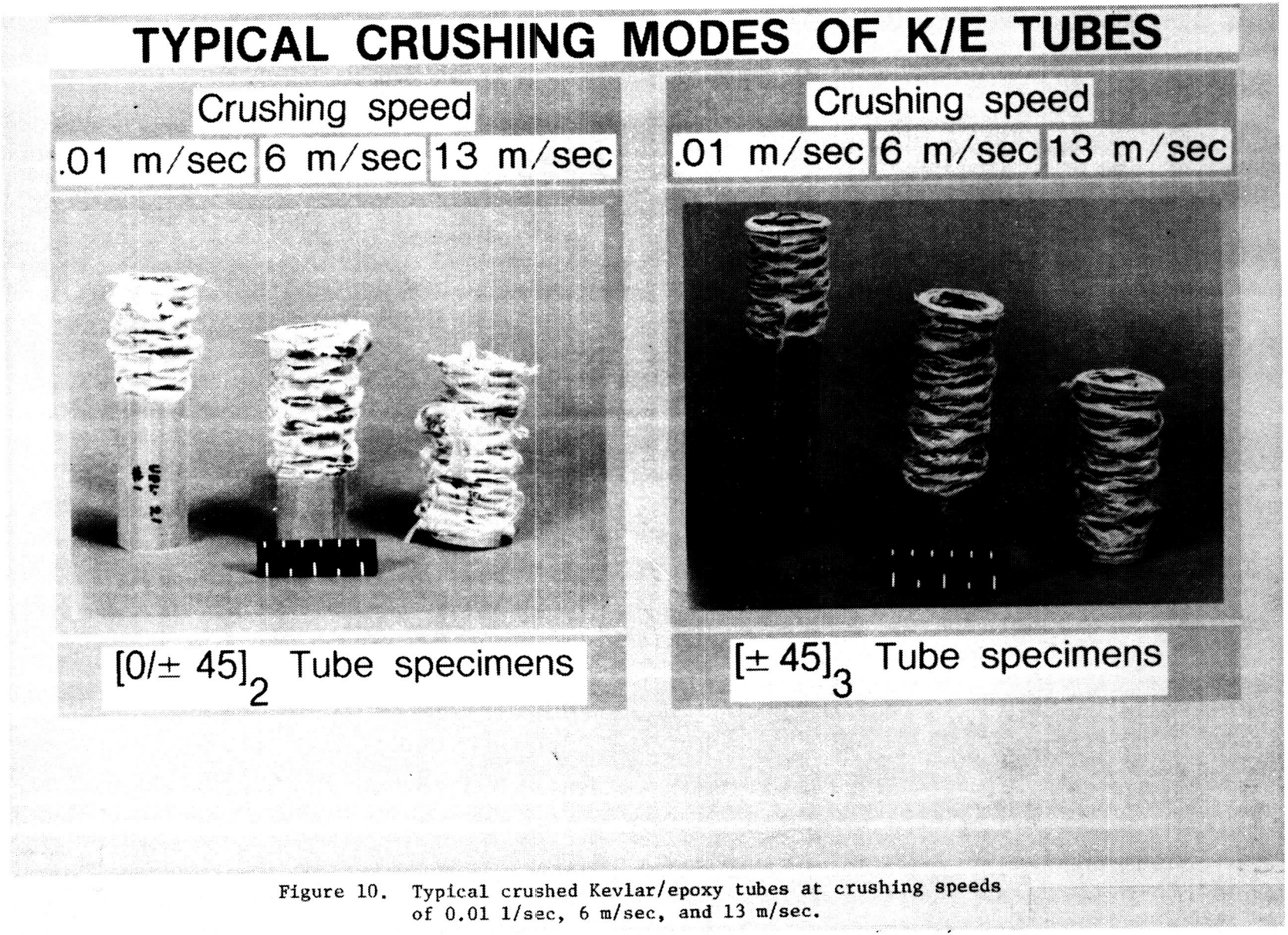

Figure 10. Typical crushed Kevlar/epoxy tubes at crushing speeds of 0.01 1/sec, 6 m/sec, and 13 m/sec.

Standard Bibliographic Page

1. Report No. NASA TM-89122 USA AVSCOM TR 87-B-1	2. Government Accession No.	3. Recipient's Catalog No.
4. Title and Subtitle THE EFFECTS OF CRUSHING SPEED ON THE ENERGY-ABSORPTION CAPABILITY OF COMPOSITE MATERIAL		5. Report Date March 1987 6. Performing Organization Code
7. Author(s) Gary L. Farley		8. Performing Organization Report No.
9. Performing Organization Name and Address NASA Langley Research Center, Hampton, VA 23665-5225 U.S. Army Aviation Research and Technology Activity (AVSCOM) Aerostructures Directorate (USAARTA) Hampton, VA 23665-5225		10. Work Unit No. 505-63-01-06 11. Contract or Grant No.
12. Sponsoring Agency Name and Address National Aeronautics and Space Administration Washington, DC 20546 U.S. Army Aviation Systems Command, St. Louis, MO 63166		13. Type of Report and Period Covered Technical Memorandum 14. Sponsoring Agency Code

15. Supplementary Notes

Gary L. Farley, U.S. Army Aerostructures Directorate, USAARTA-AVSCOM, Langley Research Center, Hampton, Virginia.

16. Abstract

The energy-absorption capability as a function of crushing speed was determined for Thornel 300/Fiberite 934 (Gr/E) and Kevlar-49/Fiberite 934 (K/E) composite material. Circular cross section tube specimens were crushed at quasi-static, 6 m/sec, and 12 m/sec speeds. Ply orientations of the tube specimens were $[0/\pm\theta]_2$ and $[\pm\theta]_3$ where θ = 15, 45, and 75 degrees. Based upon the results of these tests the energy-absorption capability of Gr/E and K/E was determined to be a function of crushing speed. The crushing modes based upon exterior appearance of the crushed tubes were unchanged for either material. However, the interlaminar crushing behavior changed with crushing speed.

17. Key Words (Suggested by Authors(s))	18. Distribution Statement
Impact Graphite Kevlar Crushing Speed Energy-Absorption Composite Material	Unclassified - Unlimited Subject Category 24

19. Security Classif.(of this report)	20. Security Classif.(of this page)	21. No. of Pages	22. Price
Unclassified	Unclassified	21	A02

For sale by the National Technical Information Service, Springfield, Virginia 22161